



Contents lists available at ScienceDirect

Journal of Advanced Research

journal homepage: [www.elsevier.com/locate/jare](http://www.elsevier.com/locate/jare)

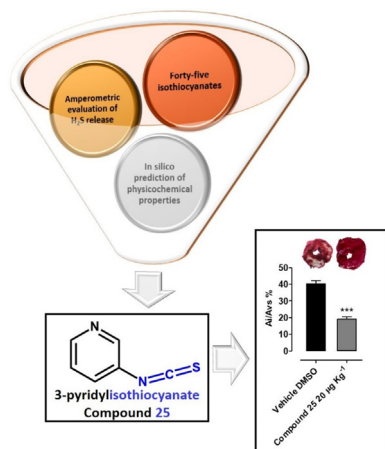
## Structure-activity relationships study of isothiocyanates for H<sub>2</sub>S releasing properties: 3-Pyridyl-isothiocyanate as a new promising cardioprotective agent

Valentina Citi<sup>a</sup>, Angela Corvino<sup>b</sup>, Ferdinando Fiorino<sup>b</sup>, Francesco Frecentese<sup>b</sup>, Elisa Magli<sup>b</sup>, Elisa Perissutti<sup>b</sup>, Vincenzo Santagada<sup>b</sup>, Simone Brogi<sup>a</sup>, Lorenzo Flori<sup>a</sup>, Era Gorica<sup>a</sup>, Lara Testai<sup>a</sup>, Alma Martelli<sup>a</sup>, Vincenzo Calderone<sup>a,\*</sup>, Giuseppe Caliendo<sup>b,\*</sup>, Beatrice Severino<sup>b</sup>

<sup>a</sup> Department of Pharmacy, University of Pisa, Via Bonanno, 6, I-56126 Pisa, Italy

<sup>b</sup> Department of Pharmacy, School of Medicine, University of Naples «Federico II», Via D. Montesano, 49, 80131 Napoli, Italy

### GRAPHICAL ABSTRACT



### ARTICLE INFO

#### Article history:

Received 13 January 2020

Revised 27 February 2020

Accepted 29 February 2020

Available online xxxx

#### Keywords:

Hydrogen sulfide

H<sub>2</sub>S releasing compounds

Isothiocyanates

*In silico* prediction

Cardioprotection

### ABSTRACT

A library of forty-five isothiocyanates, selected for their different chemical properties, has been evaluated for its hydrogen sulfide (H<sub>2</sub>S) releasing capacity. The obtained results allowed to correlate several factors such as steric hindrance, electronic effects and position of the substituents to the observed H<sub>2</sub>S production. Moreover, the chemical-physical profiles of the selected compounds have been studied by an *in silico* approach and from a combination of the obtained results, 3-pyridyl-isothiocyanate (**25**) has been selected as the most promising one. A detailed pharmacological characterization of its cardioprotective action has been performed. The results herein obtained strongly indicate 3-pyridyl-isothiocyanate (**25**) as a suitable pharmacological option in anti-ischemic therapy.

© 2020 Production and hosting by Elsevier B.V. on behalf of Cairo University. This is an open access article under the CC BY-NC-ND license (<http://creativecommons.org/licenses/by-nc-nd/4.0/>).

Peer review under responsibility of Cairo University.

\* Corresponding authors.

E-mail addresses: [caliendo@unina.it](mailto:caliendo@unina.it) (V. Calderone), [vincenzo.calderone@unipi.it](mailto:vincenzo.calderone@unipi.it) (G. Caliendo).

<https://doi.org/10.1016/j.jare.2020.02.017>

2090-1232/© 2020 Production and hosting by Elsevier B.V. on behalf of Cairo University.

This is an open access article under the CC BY-NC-ND license (<http://creativecommons.org/licenses/by-nc-nd/4.0/>).

Please cite this article as: V. Citi, A. Corvino, F. Fiorino et al., Structure-activity relationships study of isothiocyanates for H<sub>2</sub>S releasing properties: 3-Pyridyl-isothiocyanate as a new promising cardioprotective agent, Journal of Advanced Research, <https://doi.org/10.1016/j.jare.2020.02.017>

## Introduction

The gasotransmitter hydrogen sulphide ( $H_2S$ ), an endogenous ubiquitous signalling molecule, is known for its beneficial effects on different mammalian systems [1].  $H_2S$  is mainly produced from L-Cysteine via the catalytic activity of two pyridoxal-5'-phosphate dependent enzymes, known as cystathionine- $\beta$ -synthase (CBS) and cystathionine- $\gamma$ -lyase (CSE) [2]. A third pathway, where 3-mercaptopyruvate sulphur transferase (3-MST) and cysteine aminotransferase (CAT) [3–5] cooperate, is also responsible for  $H_2S$  biosynthesis. Endogenous  $H_2S$  is involved in many physiological processes and the role of  $H_2S$  has been mostly studied by inhibiting its physiological production [6,7] or using exogenous sources of  $H_2S$ .

$H_2S$  exhibits cardioprotective activity against ischemia/reperfusion (I/R) or hypoxic injury. The mechanisms of action accounting for this cardioprotective activity involve mitochondrial ATP-sensitive potassium channels (mitoKATP) [8], anti-apoptotic responses [9] and inhibition of type-5 phosphodiesterase [10]. Furthermore,  $H_2S$  behaves as an antioxidant molecule, able to activate the Nrf-2-mediated machinery and reduce the reactive oxygen species, suggesting that also this effect may be involved in the protective properties against I/R injury [11].

Due to the intriguing biological activities of  $H_2S$  in the cardiovascular function, compounds able to generate exogenous  $H_2S$ , are viewed as promising cardioprotective agents. In this scenario, different classes of  $H_2S$ -donors have been described in the literature, such as GYY4137 [12], thiadiazolidin-3,5-diones [13], arylthioamides [14], iminothioethers [15], mercaptopyruvate [16], dithioates [17]. Furthermore, also natural [18,19] and synthetic [20] isothiocyanates are known to generate  $H_2S$  with a slow kinetic and in an L-Cysteine dependent manner. In addition, hybrid molecules bringing an isothiocyanate portion were developed and investigated in neurodegenerative diseases [21–23].

Despite their numerous properties, natural isothiocyanates have some limitations: most of them, including sulforaphane, are volatile oils and particularly unstable at room temperature. In fact, they are spontaneously converted into several inactive intermediates with relatively high degradation rates [24].

Starting from these findings [25,26], we selected a series of natural and synthetic isothiocyanates, aiming at defining a structure-activity relationship correlating their structure and  $H_2S$ -releasing properties. We selected forty-five aliphatic and aromatic isothiocyanates, commercially available, variously substituted both in terms of steric hindrance and electronic properties. Aromatic derivatives included compounds with electron-withdrawing and electron-donating substituents in *ortho*, *meta* and *para* positions with respect to the -SCN moiety. Pyridine (25) and naphthalene (37) derivatives were selected as ring equivalents of phenyl isothiocyanate (1). Among the selected compounds, 3-pyridyl-isothiocyanate (25) showed the highest  $H_2S$  releasing ability. This compound has been employed in a different research field as starting material for the synthesis of cationic polymers for targeted delivery [27,28]. Here we describe it as an efficient  $H_2S$  donor that was thoroughly studied for its pharmacological activity in different experimental models of I/R injury in rats.

## Materials and methods

### Substances

All isothiocyanates were commercial products purchased from Fluorochem (Hadfield, UK).

### Amperometric approach

The  $H_2S$ -generating properties of the tested compounds have been evaluated by an amperometric approach, through an Apollo-4000 Free Radical Analyzer (WPI) detector and  $H_2S$ -selective mini-electrodes at room temperature, in phosphate buffer solution at pH 7.4 in the absence or in the presence of L-cysteine 4 mM, as reported previously [18]. The generation of  $H_2S$  was observed for 30 min.

### Molecules preparation and prediction of physicochemical properties

The three-dimensional structures of the selected molecules were built in Maestro molecular modelling environment (Maestro release 2018) and minimized using MacroModel software (MacroModel, Schrödinger, LLC, New York, NY, 2018) as previously described [28,29]. Furthermore, LigPrep (LigPrep, Schrödinger, LLC, New York, NY, 2018) application was used to refine the chemical structures. The resulting compounds, saved as sdf file, were investigated for their physicochemical properties. This investigation was performed by the webserver FAFDrugs4.0 (<http://fafdrugs4.mti.univ-paris-diderot.fr/> access May 2019) [30].

### Compound 25 intracellular $H_2S$ release measurement

H9c2 were cultured up to about 90% confluence and 24 h before the experiment cells were seeded onto a 96 well clear bottom black plate at a density of  $72 \times 10^3$  per well. After 24 h, the medium was replaced and cells were incubated for 30 min with a 100  $\mu$ M solution of the fluorescent dye WSP-1 (Washington State Probe, 1,3'-methoxy-3-oxo-3H-spiro[isobenzofuran-1,9'-xanthen]-6'-yl 2-(pyridine-2-yl-disulfanyl benzoate) that is highly sensitive for  $H_2S$  detection [31,32]. Then, the supernatant was removed and replaced with different solutions of compound 25 dissolved in standard buffer (HEPES 20 mM; NaCl, 120 mM; KCl, 2 mM;  $CaCl_2 \cdot 2H_2O$ , 2 mM;  $MgCl_2 \cdot 6H_2O$ , 1 mM; glucose, 5 mM; and pH 7.4, at room temperature) at three increasing concentrations (30, 100, and 300  $\mu$ M). The change in fluorescence (expressed as fluorescence index measured at  $\lambda = 465\text{--}515$  nm) was monitored every 5 min for 60 min, by means of a spectrofluorometer. On the bases of previous experiments [15,33], 4-carboxyphenylisothiocyanate (4-CPI, Sigma-Aldrich) 300  $\mu$ M was used as slow  $H_2S$  donor reference compound. Six different experiments ( $n = 6$ ) were performed, each carried out in three replicates. The results are expressed as mean  $\pm$  SEM.

### Animal procedures and ethical statements

All the procedures involving animals were carried out following the guidelines of the European Community Council Directive 86-609 and in accordance with the Code of Ethics of the World Medical Association (Declaration of Helsinki, EU Directive 2010/63/EU for animal experiments). All the experiments were authorized by the Ethical Committee of the University of Pisa and by the Italian Ministry of Health (authorization number 45972/2016). All the animals were housed in humidity- and temperature-controlled rooms (22 °C and 50%, respectively) with 12 h light/dark cycles, water, and food availability ad libitum.

### Measurement of coronary flow

Adult male normotensive Wistar rats (300–350 g) were anaesthetized with an overdose of sodium thiopental (100  $mg \cdot kg^{-1}$  i. p.); hearts were quickly excised, rapidly mounted in a Langendorff apparatus (Radnoti, Monrovia, USA) and perfused with Krebs solution ( $NaHCO_3$ , 25 mM; NaCl, 118.1 mM; KCl, 4.8 mM;  $MgSO_4$ ,

1.2 mM; CaCl<sub>2</sub>·2H<sub>2</sub>O, 1.6 mM; KH<sub>2</sub>PO<sub>4</sub>, 1.2 mM; and glucose, 11.5 mM) gassed with cloxcarb at 37 °C at constant pressure (70–80 mmHg). As reported previously [34], coronary flow (CF) was volumetrically recorded every 5 min, expressed as mL·min<sup>-1</sup>, and normalized to the heart weight (g). After a 20 min equilibration period, some hearts were selected to determine the effects of compound **25** on CF of hearts precontracted with angiotensin II (AngII). These hearts were perfused with AngII 0.1 μM, and at the onset of a stable coronary spasm (observed as a reduction in the CF), cumulatively increasing concentrations of compound **25** (1, 3, 10 and 30 μM, for 20 min) were perfused (in the constant presence of AngII 0.1 μM). Changes in CF are expressed as percentage (%) of the basal CF. Experiments were carried out on hearts from six animals (n = 6) for each different treatment.

#### Ex vivo ischemia/reperfusion injury

Male Wistar rats (260–350 g) were randomized in 8 groups and were treated with an intra peritoneal (i.p.) injection of different increasing doses of compound **25** 180 μg·kg<sup>-1</sup>, 60 μg·kg<sup>-1</sup>, 20 μg·kg<sup>-1</sup> and 6.7 μg·kg<sup>-1</sup> or diazoxide 40 mg·Kg<sup>-1</sup> (a mitoK<sub>ATP</sub> opener) or 4-CPI 240 μg·Kg<sup>-1</sup> or vehicle (DMSO) or 5-hydroxy decanoic acid (5-HD) 10 mg·kg<sup>-1</sup> for 20 min followed by compound **25** 20 μg·kg<sup>-1</sup>. After 2 h, all the animals were anaesthetized with sodium thiopental (100 mg·kg<sup>-1</sup> i.p.) and heparinized (100UI i.p.) to prevent blood clotting. After opening the chest, hearts were quickly excised, mounted on a Langendorff apparatus as reported previously. A water-filled latex balloon connected to a pressure transducer (Bentley Trantec, mod 800, UgoBasile, Comerio, Italy) was introduced into the left ventricle via the mitral valve and the volume was adjusted to achieve a stable left ventricular end-diastolic pressure of 5–10 mmHg during initial equilibration. After 30 min of equilibration, hearts were subjected to 30 min of global ischemia (no flow). Thereafter, hearts were perfused for 120 min. Functional parameters were continuously recorded during the whole experiment. At the end of reperfusion hearts were removed from the Langendorff apparatus and left ventricles were isolated and submitted to morphometric assays. Experiments were carried out on hearts from six animals (n = 6) for each different treatment.

#### Morphometric analysis of the ischemic area

The potential cardioprotective effects of compound **25** have been evaluated by the possible reduction of the size of injured areas in compound **25**-treated hearts submitted to I/R. The left ventricle was cut in 2 mm-wide slices which were immersed in a 1% aqueous solution of 2,3,5-triphenyltetrazolium chloride (TTC) for 20 min at 37 °C and then in a 10% aqueous solution of formaldehyde. After 24 h, ventricular slices were photographed and analysed to highlight necrotic areas due to the ischemic process (visible as a white or light pink color) and the healthy areas (visible as a strong red due to the TTC reaction).

#### LDH activity measurement

The LDH was measured for dynamic monitoring of cellular damage with the experiments lasting 120 min of reperfusion. Coronary effluent samples were collected at the last 5 min of the pre-ischemic phase and every 5 min during the first 30 min of reperfusion and then every 10 min—a total of 13 samples were collected per heart. The flow rate was measured each time an LDH sample was collected. The samples were stored on ice until the end of each experiment. The LDH was assessed by a spectrophotometric method, by adding 27.6 mM pyruvate and 4.8 mM NADH, and measuring the conversion of NADH to NAD<sup>+</sup> at the wavelength of λ = 340 nm. The amount of released LDH has been expressed in

enzymatic mU·g<sup>-1</sup> released in 120 min of reperfusion (without the small amount recorded in the pre-ischemic phase), resulting from the AUC analysis (area under the curve of the LDH amount recorded) and related to 1 g of the heart weight.

#### Acute in vivo myocardial infarction

The cardioprotective effects of compound **25** were evaluated *in vivo*, in an experimental model more closely resembling the clinical condition of acute myocardial infarction. The experimental protocol for coronary occlusion-reperfusion was performed as described previously [35], with minor modifications. Two hours before the experimental procedure, rats received an i.p. injection (about 0.3 mL) of compound **25** (20 μg·kg<sup>-1</sup>) or diazoxide 40 mg·Kg<sup>-1</sup> (a mitoK<sub>ATP</sub> opener) or 4-CPI 240 μg·Kg<sup>-1</sup> or vehicle (DMSO). Then, rats were anaesthetized with sodium thiopental (70 mg·kg<sup>-1</sup>, i.p.). The trachea was intubated and connected to a rodent ventilator (mod. 7025 UgoBasile, Comerio, Italy) for artificial ventilation with room air (stroke volume, 1 mL/100 g body weight; 70 S/min). Electrocardiogram (ECG) was continuously measured by lead II (Mindray, PM5000, 2 Biological Instruments, Varese, Italy). The chest was opened by a left thoracotomy. A 6–0 surgical needle was passed around the left anterior descending coronary artery (LAD), located between the base of the pulmonary artery and left atrium. The ends of the suture were passed through a polypropylene tube (PE50) to form a snare, allowing reversible artery occlusion. The acute infarction protocol consisted of 30 min occlusion/120 min reperfusion; successful occlusion was confirmed by observing regional cyanosis downstream of the ligation, and by ST elevation in the ECG recording. At the end of reperfusion, rats were euthanized by an overdose of sodium thiopental, hearts were quickly excised, mounted on a Langendorff apparatus and perfused for 10 min with Krebs solution at 37 °C to clean coronary blood vessels. Then, the atria and right ventricle were removed from the hearts. The left ventricular tissue was dried, frozen at –20 °C, and cut into 4–5 transverse slices from apex to base of equal thickness (about 2 mm). The slices were submitted to morphometric analysis. Experiments were carried out on hearts from six animals (n = 6) for each different treatment.

## Results

#### Amperometric determination of H<sub>2</sub>S release

The compounds selected comprehend both aliphatic and aromatic isothiocyanates characterized by different substituents (electron donating/withdrawing and different steric hindrance groups). All the compounds were incubated at the concentration of 1 mM in the presence or in the absence of L-Cys 4 mM to evaluate their H<sub>2</sub>S releasing properties. The results about the amount of H<sub>2</sub>S produced are expressed as C<sub>max</sub> in μM (maximal concentration of H<sub>2</sub>S at the steady state) and are listed in Table 1.

The incubation in the assay buffer without L-cysteine led to a negligible or very low release of H<sub>2</sub>S (C<sub>max</sub> < 2 μM; Table 1) for most of the compounds. Following L-cysteine addition, the H<sub>2</sub>S release is, generally, more significant with the highest C<sub>max</sub> value of 65.436 μM (compound **25**).

Referring to the L-cysteine evoked H<sub>2</sub>S release, the structure-activity relationships, relative to the selected compounds, can be described as follows. As a general trend, the aromatic compounds were more efficient donors with respect to the aliphatic ones. The greater ability to release H<sub>2</sub>S is associated with the presence on the aromatic ring of electron-withdrawing groups with a fairly linear trend observable in the series of *ortho*-*meta*- and *para*-substituted compounds:

**Table 1**  
Structures and parameters of  $C_{max}$  of the forty-five isothiocyanates (1 mM) were determined after incubation in the assay buffer at physiological pH and temperature, in the absence or in presence of 4 mM L-Cysteine.

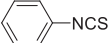
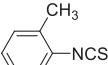
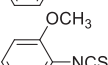
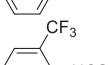
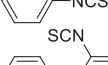
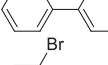
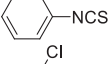
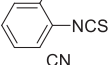
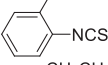
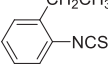
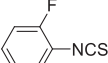
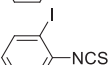
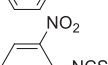
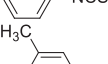
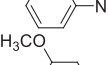
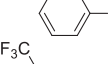
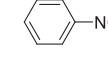
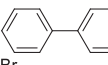
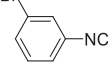
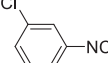
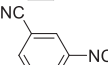
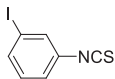
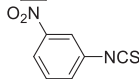
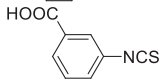
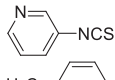
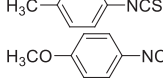
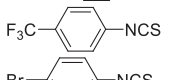
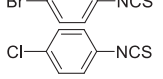
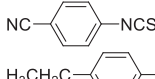
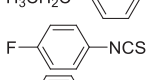
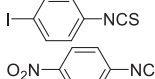
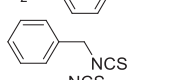
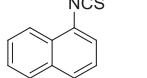
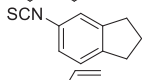
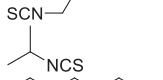
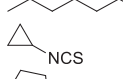
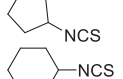
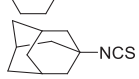
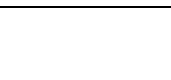
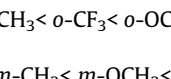
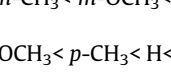
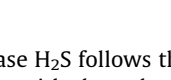
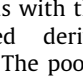
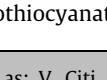
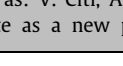
Compd	Structure	H <sub>2</sub> S-release without L-cysteine 4 mM ( $C_{max}$ $\mu$ M)	H <sub>2</sub> S-release + L-cysteine ( $C_{max}$ $\mu$ M)
1		1.214 $\pm$ 0.145	10.029 $\pm$ 1.206
2		1.041 $\pm$ 0	2.396 $\pm$ 0.515
3		2.386 $\pm$ 0.974	5.270 $\pm$ 0.557
4		0.364 $\pm$ 0	4.154 $\pm$ 0.537
5		0	0.29 $\pm$ 0.02
6		3.617 $\pm$ 1.030	13.335 $\pm$ 1.863
7		0	18.309 $\pm$ 2.220
8		0	6.33 $\pm$ 1.51
9		0	0.16 $\pm$ 0.01
10		5.351 $\pm$ 0	23.406 $\pm$ 3.506
11		0	1.93 $\pm$ 0.14
12		0.614 $\pm$ 0.267	20.066 $\pm$ 0.337
13		0.411 $\pm$ 0	5.732 $\pm$ 0.929
14		0.865 $\pm$ 0.303	6.422 $\pm$ 0.551
15		0.168 $\pm$ 0	19.028 $\pm$ 1.328
16		0	0.15 $\pm$ 0.02
17		5.355 $\pm$ 1.521	17.750 $\pm$ 2.961
18		0	21.575 $\pm$ 1.220
19		0	29.29 $\pm$ 1.85
20		0	1.2 $\pm$ 0.9
21		3.594 $\pm$ 0	36.919 $\pm$ 4.399

Table 1 (continued)

Compd	Structure	H <sub>2</sub> S-release without L-cysteine 4 mM (C <sub>max</sub> μM)	H <sub>2</sub> S-release + L-cysteine (C <sub>max</sub> μM)
22		0	2.47 ± 0.14
23		0.912 ± 0.432	22.158 ± 1.857
24		0.59 ± 0.38	30.32 ± 1.37
25		8.719 ± 1.555	65.436 ± 4.356
26		0.612 ± 0	9.064 ± 0.444
27		1.550 ± 0.441	7.411 ± 0.126
28		0.786 ± 0	32.007 ± 3.404
29		5.350 ± 1.000	37.713 ± 4.866
30		1.876 ± 0	17.576 ± 2.997
31		0	16.58 ± 0.32
32		0	3.87 ± 0.42
33		3.777 ± 0	19.517 ± 1.194
34		0	1.19 ± 0.27
35		0.635 ± 0.369	24.880 ± 4.449
36		0	1.246 ± 0.891
37		0.205 ± 0.005	0.36 ± 0.03
38		0	2.08 ± 0.05
39		0.674 ± 0.286	1.124 ± 1.015
40		0	0
41		2.541 ± 0.585	12.973 ± 0.981
42		1.389 ± 0.586	0
43		4.092 ± 0.413	0
44		0.161 ± 0	0.461 ± 0
45		0	0

*o*-CH<sub>2</sub>CH<sub>3</sub> < *o*-I < *o*-CH<sub>3</sub> < *o*-CF<sub>3</sub> < *o*-OCH<sub>3</sub> < *o*-CN < H < *o*-Br < *o*-Cl < *o*-NO<sub>2</sub> < *o*-F  
*m*-CH<sub>2</sub>CH<sub>3</sub> < *m*-I < *m*-CH<sub>3</sub> < *m*-OCH<sub>3</sub> < H < *m*-Br < *m*-CF<sub>3</sub> < *m*-Cl < *m*-NO<sub>2</sub> < *m*-CN < *m*-F  
*p*-I < *p*-CH<sub>2</sub>CH<sub>3</sub> < *p*-OCH<sub>3</sub> < *p*-CH<sub>3</sub> < H < *p*-CN < *p*-Cl < *p*-F < *p*-NO<sub>2</sub> < *p*-CF<sub>3</sub> < *p*-Br

The ability to release H<sub>2</sub>S follows the order *ortho* < *meta* < *para* for all the compounds with the only exception of chloro-, fluoro- and iodo-substituted derivatives that follow the order *para* < *ortho* < *meta*. The poor H<sub>2</sub>S releasing profile of the *o*-, *m*- and *p*-iodo-phenylisothiocyanates results from the combination

of steric factors (particularly important for the *ortho*- and *meta*-derivatives) and reactivity features. Aryl iodide, in fact, are very prone to C-S cross-coupling with aromatic and aliphatic thiols.

The most efficacious H<sub>2</sub>S donor was compound **25**, 3-pyridyl-isothiocyanate, where the electron-deficient nature of the pyridine ring, attributed to the electron-withdrawing, inductive, and mesomeric effects of the nitrogen atom, accounts for the high H<sub>2</sub>S release. The molecular mechanism responsible for thiol activated H<sub>2</sub>S release from isothiocyanate has been recently elucidated in detail [36]. It involves an intramolecular cyclization of the cysteine-ITC intermediate crucial for the H<sub>2</sub>S releasing. The strongly electrophilic nature of the -SCN moiety is amplified by

the presence of electron-withdrawing groups on the aromatic ring thus making the central carbon more prone to undergo a nucleophilic attack.

#### *In silico* evaluation of physicochemical properties

The drug-like profile represents a critical property for assuring the advancement of a drug candidate into preclinical studies and clinical trials. Notably, at the beginning of drug discovery trajectory it is particularly important to prioritize potential hit compounds that could be suitable starting points for searching novel drug candidates. Accordingly, it is a common procedure, during the drug discovery pipeline, consider some molecular descriptors for selecting potential drug candidates with satisfactory physicochemical properties and ADMET (absorption, distribution, metabolism, excretion, and toxicity) profile [29,37–39]. Accordingly, we performed an *in silico* analysis to determine which derivatives could be submitted to further cellular and *in vivo* studies. The calculation of the physicochemical properties, regarding the mole-

cules reported in Table 1, was performed by means of the online server FAFDrugs4.0 and the output is reported in Table 2.

The calculation of the physicochemical properties of the molecules, along with some filters commonly used in pharma companies highlighted a conserved trend indicating that the selected compounds possess a satisfactory drug-like profile, although some properties can be improved including chemical complexity. According to this calculation all the compounds presented no violation of the Lipinski rules of five [40]. The analysis of the main PhysChem descriptors is reported in Fig. 1A.

The computational analysis revealed that for solubility issue compounds **5**, **16**, **22**, **37** and **38** cannot be considered for further investigation. Moreover, also compounds **11**, **15**, **17**, **28** and **34**, presenting a calculated solubility under 4000 mg·L<sup>-1</sup>, were not considered for additional pharmacological tests. The remaining compounds, although with different values, showed satisfactory solubility according to the different descriptors used in the calculation (Table 2). Supplementary analysis considering two filters used in Pharma companies (GSK 4\_400 filter is related to the

**Table 2**  
*In silico* drug-like profile of the molecules presented in this work.

Compd	MW <sup>a</sup>	logP <sup>b</sup>	logSw <sup>c</sup>	tPSA <sup>d</sup>	Lipinski <sup>e</sup>	Solubility (mg L <sup>-1</sup> )	Solubility FI <sup>f</sup>	VEBER <sup>g</sup>	EGAN <sup>h</sup>	4_400 <sup>i</sup>	3_75 <sup>j</sup>
1	135.19	3.40	-3.07	44.45	0	6267	Good	Good	Good	Good	Bad
2	149.21	3.69	-3.28	44.45	0	5587	Good	Good	Good	Good	Bad
3	165.21	3.29	-3.05	53.68	0	7811	Good	Good	Good	Good	Bad
4	203.18	4.21	-3.88	44.45	0	4191	Good	Good	Good	Good	Bad
5	211.28	4.95	-4.51	44.45	0	2332	Reduced	Good	Good	Good	Bad
6	214.08	4.01	-3.94	44.45	0	4144	Good	Good	Good	Good	Bad
7	169.63	3.95	-3.63	44.45	0	4492	Good	Good	Good	Good	Bad
8	160.20	3.04	-2.98	68.24	0	8150	Good	Good	Good	Good	Bad
9	163.24	4.12	-3.54	44.45	0	4747	Good	Good	Good	Good	Bad
10	153.18	3.42	-3.20	44.45	0	6272	Good	Good	Good	Good	Bad
11	261.08	3.97	-4.21	44.45	0	3872	Good	Good	Good	Good	Bad
12	180.18	3.15	-3.09	90.27	0	8282	Good	Good	Good	Good	Bad
13	149.21	3.72	-3.30	44.45	0	5482	Good	Good	Good	Good	Bad
14	165.21	3.68	-3.30	53.68	0	6109	Good	Good	Good	Good	Bad
15	203.18	4.37	-3.98	44.45	0	3789	Good	Good	Good	Good	Bad
16	211.28	4.99	-4.53	44.45	0	2274	Reduced	Good	Good	Good	Bad
17	214.08	4.12	-4.01	44.45	0	3866	Good	Good	Good	Good	Warning
18	169.63	3.36	-3.26	44.45	0	6514	Good	Good	Good	Good	Bad
19	160.20	3.13	-3.04	68.24	0	7700	Good	Good	Good	Good	Bad
20	163.24	4.16	-3.56	44.45	0	4629	Good	Good	Good	Good	Bad
21	153.18	3.53	-3.26	44.45	0	5852	Good	Good	Good	Good	Bad
22	261.08	4.94	-4.82	44.45	0	2101	Reduced	Good	Good	Good	Bad
23	180.18	3.26	-3.16	90.27	0	7672	Good	Good	Good	Good	Warning
24	179.20	2.96	-2.94	84.58	0	9426	Good	Good	Good	Good	Good
25	136.17	2.25	-2.38	57.34	0	12,637	Good	Good	Good	Good	Warning
26	149.21	3.92	-3.43	44.45	0	4833	Good	Good	Good	Good	Bad
27	165.21	3.58	-3.23	53.68	0	6507	Good	Good	Good	Good	Bad
28	203.18	4.44	-4.03	44.45	0	3625	Good	Good	Good	Good	Bad
29	214.08	4.03	-3.96	44.45	0	4092	Good	Good	Good	Good	Bad
30	169.63	3.91	-3.61	44.45	0	4606	Good	Good	Good	Good	Bad
31	160.20	3.06	-2.99	68.24	0	8048	Good	Good	Good	Good	Bad
32	163.24	4.35	-3.68	44.45	0	4107	Good	Good	Good	Good	Bad
33	153.18	3.44	-3.21	44.45	0	6194	Good	Good	Good	Good	Bad
34	261.08	4.22	-4.37	44.45	0	3308	Good	Good	Good	Good	Bad
35	180.18	3.62	-3.38	90.27	0	6115	Good	Good	Good	Good	Warning
36	149.21	3.16	-2.89	44.45	0	8333	Good	Good	Good	Good	Bad
37	185.24	4.34	-4.03	44.45	0	3303	Reduced	Good	Good	Good	Bad
38	185.24	4.34	-4.03	44.45	0	3303	Reduced	Good	Good	Good	Bad
39	99.15	2.41	-1.84	44.45	0	15,731	Good	Good	Good	Good	Warning
40	101.17	2.37	-1.89	44.45	0	15,217	Good	Good	Good	Good	Warning
41	143.25	3.98	-2.91	44.45	0	7838	Good	Good	Good	Good	Bad
42	99.15	2.12	-1.72	47.69	0	17,678	Good	Good	Good	Good	Warning
43	127.21	2.83	-2.35	44.45	0	12,185	Good	Good	Good	Good	Warning
44	141.23	3.38	-2.78	44.45	0	8770	Good	Good	Good	Good	Bad
45	193.31	4.24	-3.64	44.45	0	5056	Good	Good	Good	Good	Bad

<sup>a</sup> MW: molecular weight; <sup>b</sup>logP: octanol/water partition coefficient calculated by means of XLOGP3 program; <sup>c</sup>logSw: aqueous solubility; <sup>d</sup>tPSA: topological polar surface area; <sup>e</sup>Lipinski: number of violations of Lipinski's rule of five (up to 1 violation is allowed); <sup>f</sup>Solubility FI: solubility calculated by using the Forecaster Index (FI); <sup>g</sup>VEBER: oral bioavailability calculated by Veber rules; <sup>h</sup>EGAN: oral bioavailability calculated by Egan rules; <sup>i</sup>4\_400: safety profile calculated by the GSK 4\_400 rules; <sup>j</sup>3\_75: safety profile calculated by the Pfizer 3\_75 rules.

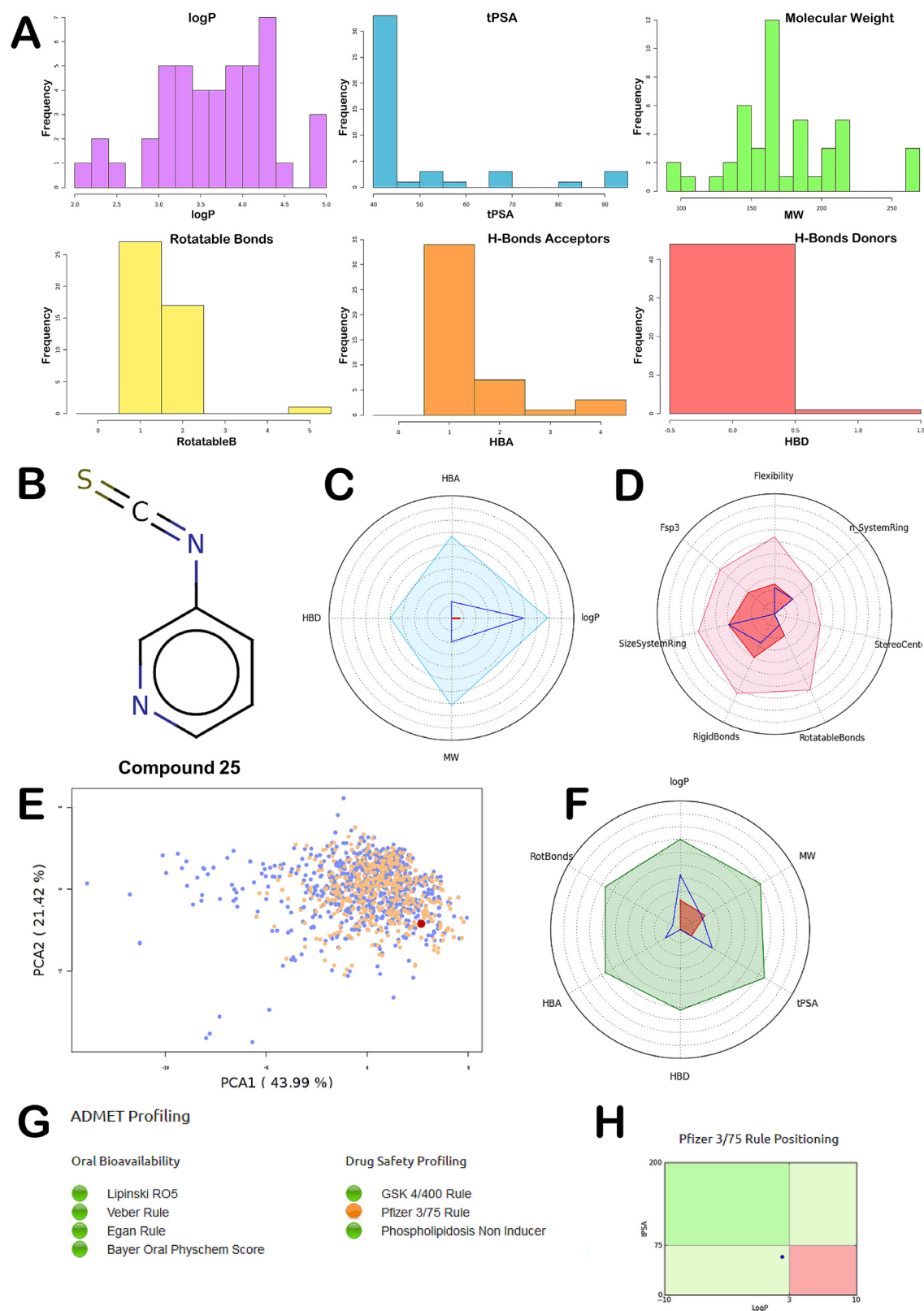


**Fig. 1.** (A) Main PhysChem descriptors analysis; (B) Chemical structure of compound 25; (C) Radar plot positioning compound's values within the selected filter ranges. Compound values (blue line) should fall within the Lipinski rule of five filter area (light blue) (pale blue and red); (D) Radar plot visualizing compound complexity. It involves the number of system ring, stereocenters, rotatable and rigid bonds, the flexibility (ration between rotatable and rigid bonds), the carbon saturation (fsp3 ratio), and the maximum size of system rings; (E) Graph regarding oral bioavailability taking into account the model obtained with 466 orally bioavailable compounds extracted from the DrugBank database and 916 orally bioavailable compounds extracted from eDrugs library. The graph is obtained by applying the PCA (Principal Component Analysis) of the 15 principal physicochemical descriptors of these molecules (blue). Then, the compound analyzed (pink) is projected, in the same conditions, on the same chemical space; (F) Radar plot representing an oral absorption estimation: The compounds values are materialized by the blue line, which should fall within the optimal green area. The white area is the extreme maximum zone while the red one is the extreme minimum zone. These zones are obtained with the following descriptors ranges: logP (-2 to 5), Molecular Weight (150-500), tPSA (20-150), Rotatable Bonds (0-10), H-Bonds Acceptors (0-10) and Donors (0-5); (G) ADMET profiling for compound 25; (H) Pfizer 3\_75 rule positioning. The output was generated by FAFDrugs4 webserver.

evaluation of logP and MW and Pfizer 3\_75 filter is related to the evaluation of logP and tPSA) allowed us to identify compounds with the best predicted drug-like profile. In particular, the GSK 4\_400 filter indicating that compounds with a logP less than 4 and a MW less than 400 Da could present a more favorable drug-like profile [41]. Instead, the Pfizer 3\_75 filter suggesting that compounds possessing a high logP value (>3) and low tPSA value (<75) are approximately 2.5 times more likely to be toxic [42]. Accordingly, all the compounds with a “bad” profile regarding these two filters were deprioritized from further investigation. Following this screening protocol, we identified a small subset of compounds (**23**, **24**, **25**, **35**, **39**, **40**, **42**, **43**) characterized by an acceptable drug-like profile. To select the candidates to submit to the pharmacological evaluation, we coupled the output of the *in silico* analysis with the data regarding the capability to release H<sub>2</sub>S. From this evaluation three compounds (**23**, **25** and **35**) were identified as suitable to proceed towards further tests; but the better H<sub>2</sub>S releasing properties and drug-like profile of **25** (Fig. 1B–H), with respect to the other two compounds, prompted us to select it for a complete pharmacological characterization.

#### Intracellular H<sub>2</sub>S release in H9c2 cells

The H<sub>2</sub>S generation was detected in H9c2 cells by spectrofluorometric measurements using the WSP-1 probe, which specifically and irreversibly interacts with H<sub>2</sub>S. The fluorescence produced by this interaction was quantitatively recorded by a spectrofluorometric approach which showed that the addition of the vehicle did not cause any significant increase of fluorescence. In contrast, the addition of compound **25** at the concentration of 30, 100 and 300 μM to H9c2, preloaded with the fluorescent dye, led to a time and concentration-dependent increase of fluorescence (FI, fluorescence index), indicating a significant generation of H<sub>2</sub>S ( $P < 0.001$  vs vehicle). 4-CPI 300 μM was used as reference H<sub>2</sub>S-donor and showed a comparable H<sub>2</sub>S-release than compound **25** 300 μM (Fig. 2).

#### Effects on the coronary flow in Angiotensin-II precontracted rat hearts

The basal CF in Langendorff-perfused rat hearts was  $10.54 \pm 0.42$  mL/min/g. As expected, the perfusion with Angiotensin II (AngII, 0.1 μM) caused a significant reduction (about 25%) of the coronary flow in isolated rat hearts when compared to the basal CF. In the

constant presence of AngII, the “add-on” perfusion with 1, 3, 10, 30 μM compound **25** led to a concentration related increase of CF up to the complete recovery of the basal coronary flow and, thus, abolishing the AngII-mediated vasoconstriction at the maximum concentration tested. 4-CPI 30 μM, used as reference H<sub>2</sub>S-donor [11], led to a slightly higher increase in the coronary flow value of about 110% (Fig. 3).

#### Effects on isolated rat heart subjected to I/R injury

I/R caused marked functional damage to isolated heart of vehicle-treated rats, with a significant reduction of myocardial vital tissue, evaluated by morphometric analysis showing about 40% of ischemic area, expressed as ratio of ischemic area to total left ventricular area ( $A_i/A_{LV}$ ). The treatment with 4-CPI 240 μg·kg<sup>-1</sup> reduced the damaged tissue of about 10% compared to vehicle. A comparable cardioprotective effect has been measured as reduction of the ischemic area in hearts of compound **25** 180 μg·kg<sup>-1</sup>-treated rats (equimolar dose of 4-CPI 240 μg·kg<sup>-1</sup>). Surprisingly, the reduction of compound **25** dose, further limited

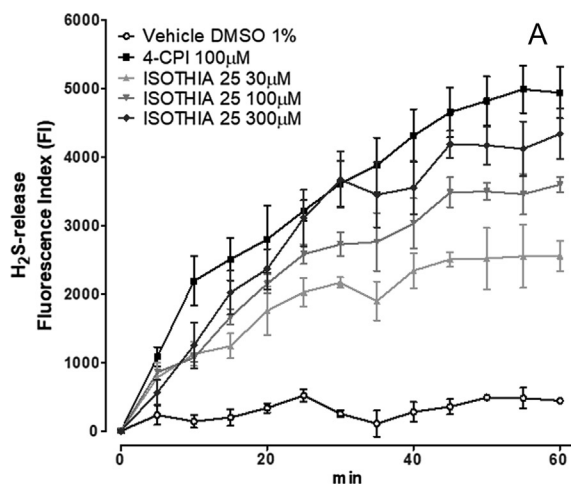


**Fig. 2.** (A) Graph shows the WSP-1 fluorescence increase evoked by the administration of vehicle (DMSO 1%), 300 μM 4-CPI, 30, 100 and 300 μM compound **25** on H9c2 cells. (B) The histograms show the total amount of H<sub>2</sub>S released by vehicle (DMSO 1%), 300 μM 4-CPI, 30, 100 and 300 μM compound **25**, during 60 min, expressed as AUC. Data are expressed as mean ± standard error. Six different experiments were carried out, each in triplicate. \*\*\* = significantly different from the vehicle ( $P < 0.001$ ).

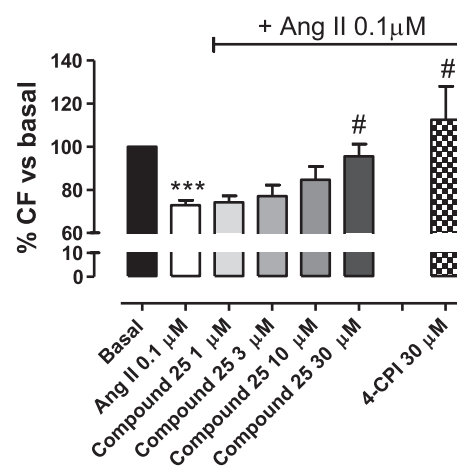
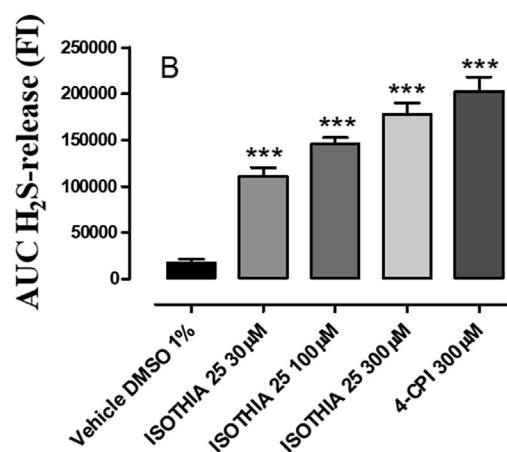


**Fig. 3.** Effects on coronary flow. The histograms show the changes of CF (expressed as a % of the basal CF) after the perfusion with 1, 3, 10, 30 μM compound **25** in the constant presence of Ang II 0.1 μM. 4-CPI 30 μM has been used as reference drug. Data are expressed as mean ± standard error. Six different experiments were carried out. \*\*\* = significantly different from basal CF ( $P < 0.001$ ); # = significantly different from Ang II 0.1 μM ( $P < 0.05$ ).





the I/R injury damage, exerting the maximum cardioprotective effect at  $20 \mu\text{g}\cdot\text{kg}^{-1}$ . Lower dose (compound **25**  $6.7 \mu\text{g}\cdot\text{kg}^{-1}$ ) lead to a reduction of the cardioprotective effect. In order to study the involvement of  $\text{mitoK}_{\text{ATP}}$  channels in the cardioprotective effects evoked by compound **25**, 5-HD  $10 \text{ mg}\cdot\text{kg}^{-1}$  has been administered 20 min before the treatment with compound **25**  $20 \mu\text{g}\cdot\text{kg}^{-1}$ : 5-HD  $10 \text{ mg}\cdot\text{kg}^{-1}$  clearly limited the cardioprotective effect of the isothiocyanate, since the ischemic area was significant more extended compared to the treatment with compound **25**  $20 \mu\text{g}\cdot\text{kg}^{-1}$  alone ( $\text{Ai}/\text{A}_{\text{LV}}\%$   $34.6 \pm 0.1$  vs  $5.3 \pm 0.5$ ; data expressed as mean  $\pm$  SEM). This result strongly suggests that  $\text{mitoK}_{\text{ATP}}$  is likely to be involved in the cardioprotective effects of  $\text{H}_2\text{S}$ . To further confirm the involvement of  $\text{mitoK}_{\text{ATP}}$  channels, administration of diazoxide  $40 \text{ mg}/\text{Kg}$  (a  $\text{mitoK}_{\text{ATP}}$  opener) imitated the ability of cardioprotective and anti-ischemic effect of compound **25** (Fig. 4).

#### LDH activity measurement

The LDH activity was measured in the coronary effluent collected during the preischemic and reperfusion periods. There were no differences between the various groups in LDH released during the preischemic period (data not shown). However, during reperfusion, LDH rose progressively in the groups treated with vehicle and with 5-HD  $10 \text{ mg}\cdot\text{kg}^{-1}$  + compound **25**  $20 \mu\text{g}\cdot\text{kg}^{-1}$ . In the perfusate of hearts from rat given compound **25** at different doses, the amount of LDH released during the reperfusion period was markedly reduced, reflecting the pattern of the  $\text{Ai}/\text{A}_{\text{LV}}\%$ . Compound **25**  $20 \mu\text{g}\cdot\text{kg}^{-1}$  was the most effective dose tested in reducing the LDH release. Diazoxide slightly reduced the amount of LDH in perfusate of hearts (Fig. 5).

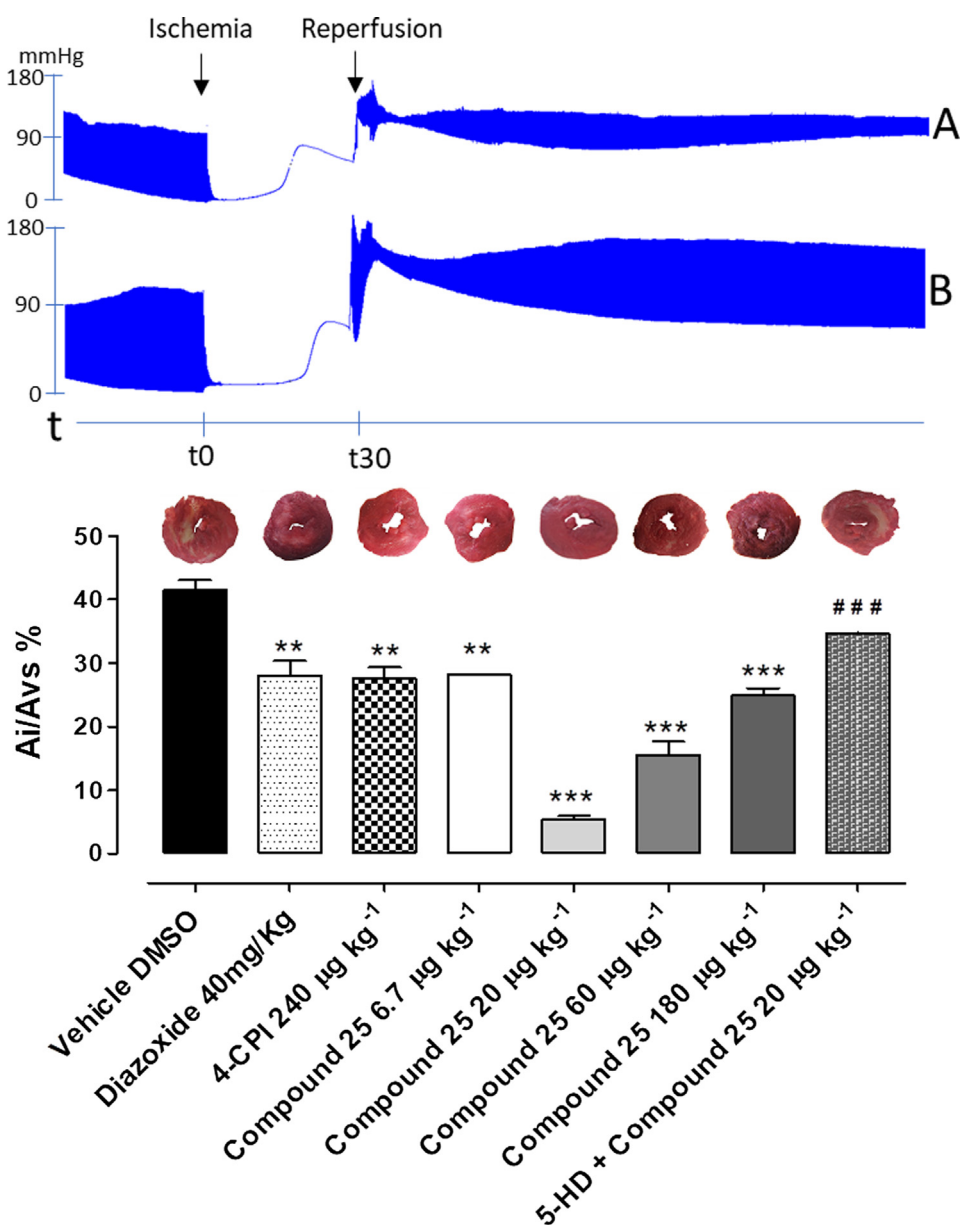


**Fig. 4.** The histograms show the morphometric analysis of the ischemic area observed in ventricular slices of rat hearts expressed as  $\text{Ai}/\text{A}_{\text{LV}}\%$  after I/R-induced injury. The bars refer to the different pharmacological pre-treatments: vehicle,  $40 \text{ mg}\cdot\text{kg}^{-1}$  diazoxide,  $240 \mu\text{g}\cdot\text{kg}^{-1}$  4-CPI,  $6.7$ ,  $20$ ,  $60$ ,  $180 \mu\text{g}\cdot\text{kg}^{-1}$  compound **25** and 5-HD  $10 \text{ mg}\cdot\text{kg}^{-1}$  +  $20 \mu\text{g}\cdot\text{kg}^{-1}$  compound **25**. Data are expressed as mean  $\pm$  standard error. Six different experiments were carried out. \* = significantly different from vehicle (\*\*\*)  $P < 0.001$ ; \*\*  $P < 0.01$ ). Representative pictures of rat left ventricle slices and the infarct size for each treatment are reported upon the histograms. Representative changes of functional parameters of vehicle (A) and compound **25**  $20 \mu\text{g}\cdot\text{kg}^{-1}$  have been reported.

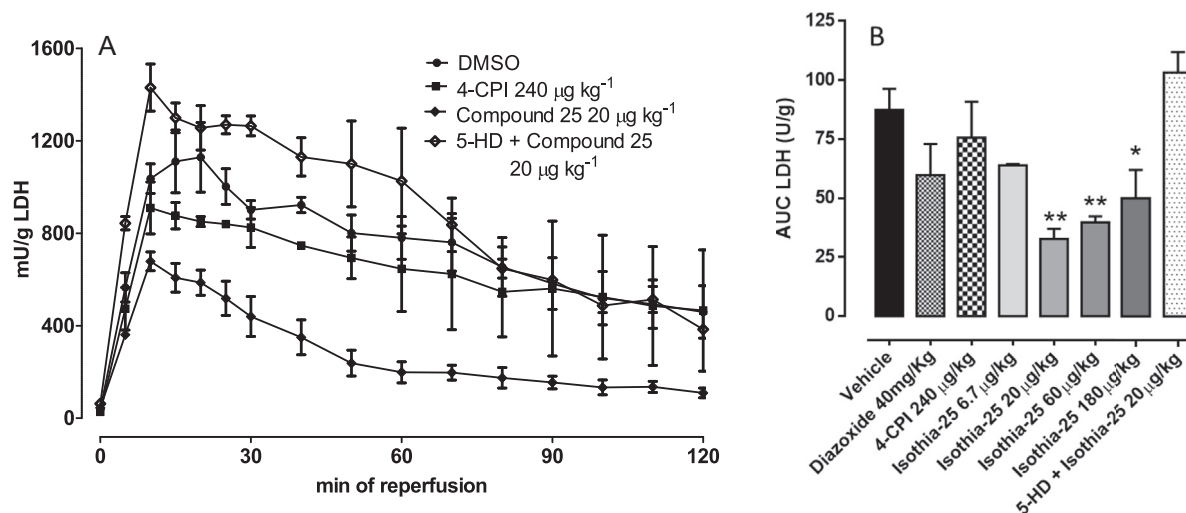


**Fig. 5.** (A) LDH release profile in rat perfused heart preparations subjected to ischemia-reperfusion obtained from rat treated with vehicle,  $240 \mu\text{g}\cdot\text{kg}^{-1}$  4-CPI,  $20 \mu\text{g}\cdot\text{kg}^{-1}$  compound **25** and  $10 \text{ mg}\cdot\text{kg}^{-1}$  5-HD +  $20 \mu\text{g}\cdot\text{kg}^{-1}$  compound **25**. (B) Bar graph shows the AUC related to LDH curves of all treatments (vehicle,  $40 \text{ mg}\cdot\text{kg}^{-1}$  diazoxide,  $240 \mu\text{g}\cdot\text{kg}^{-1}$  4-CPI, 6.7, 20, 60, 180  $\mu\text{g}\cdot\text{kg}^{-1}$  compound **25** and 5-HD  $10 \text{ mg}\cdot\text{kg}^{-1}$  +  $20 \mu\text{g}\cdot\text{kg}^{-1}$  compound **25**). Data are expressed as mean  $\pm$  standard error. Six different experiments were carried out. \* = significantly different from vehicle (\* $P < 0.05$ ; \*\* $P < 0.01$ ). # = significantly different from  $20 \mu\text{g}\cdot\text{kg}^{-1}$  compound **25** (# $P < 0.01$ ).

#### Cardioprotective effect of compound **25** in vivo

Rats were pretreated with vehicle or compound **25**  $20 \mu\text{g}\cdot\text{kg}^{-1}$  2 h before 30 min of coronary occlusion and 2 h of reperfusion. In rats treated with compound **25**  $20 \mu\text{g}\cdot\text{kg}^{-1}$ , there was a significant reduction in myocardial ischemic area, measured as  $A_i/A_{LV}\%$  ( $40.3 \pm 1.8$  vs  $19.0 \pm 1.4$ ,  $P < 0.001$ , data expressed as mean  $\pm$  SEM). These findings indicate that compound **25** exerts cardioprotective effect on I/R-induced cardiac injury. Furthermore, also the cardioprotective effects of diazoxide and 4-CPI,  $\text{mitoK}_{ATP}$  opener and the  $\text{H}_2\text{S}$ -donor reference drug respectively, have been evaluated. Both the compounds promoted a significant cardioprotection reducing the ischemic area of about 15% (Fig. 6).

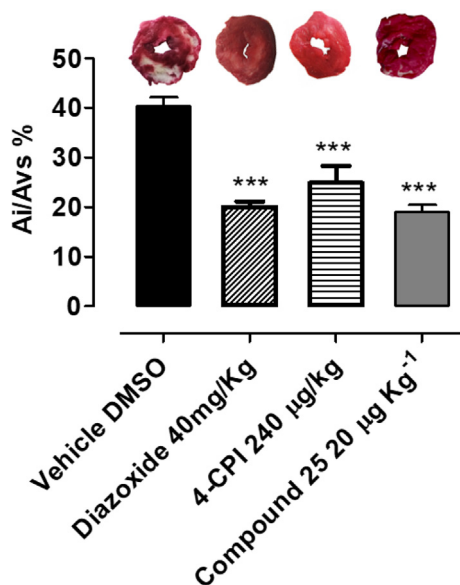


**Fig. 6.** Morphometric quantification of ischemia/reperfusion (I/R)-induced injury observed in ventricular slices of rat hearts, after acute myocardial infarction *in vivo*, after treatment with vehicle,  $40 \text{ mg}\cdot\text{kg}^{-1}$  diazoxide,  $240 \mu\text{g}\cdot\text{kg}^{-1}$  4-CPI,  $20 \mu\text{g}\cdot\text{kg}^{-1}$  compound **25**. Data are expressed as mean  $\pm$  standard error. Six different experiments were carried out. \*\*\* = significantly different from vehicle ( $P < 0.001$ ). Representative pictures of rat left ventricle slices and the infarct size for each treatment are reported upon the histograms.

#### Discussion

Infarction and myocardial ischemia are main causes of mortality in Western countries, and the identification of innovative pharmacological treatments to limit I/R-induced cardiac injury remains a challenging issue. The discovery of  $\text{H}_2\text{S}$  as an endogenous gas-transmitter and the comprehension of its pivotal role in regulating cardiovascular function and in mediating cardioprotective effect, offered novel promising perspectives in this field of research [43]. In particular,  $\text{H}_2\text{S}$ -releasing molecules, such as GYY4137 and 4-CPI, have shown significant protective effects in experimental models of myocardial I/R, suggesting that  $\text{H}_2\text{S}$ -donors can actually be viewed as a promising class of anti-ischemic drugs [44]. In this paper, we evaluated the  $\text{H}_2\text{S}$ -releasing properties of a small library of isothiocyanates, since this chemical moiety has been reported to exhibit biological effects clearly related with the release of  $\text{H}_2\text{S}$  [45]. To investigate how the structure of the isothiocyanates affects their  $\text{H}_2\text{S}$  releasing properties, several derivatives were selected and the  $\text{H}_2\text{S}$  generation was amperometrically measured.

Isothiocyanates show  $\text{l-Cys}$ -dependent  $\text{H}_2\text{S}$ -releasing properties. Accordingly, in this study we confirmed that the incubation of all the isothiocyanates led to the formation of negligible amounts of  $\text{H}_2\text{S}$  in the absence of  $\text{l-Cysteine}$ . Contrarily, in the presence of  $\text{l-Cysteine}$ , the incubation of the tested compounds led to a slow release of  $\text{H}_2\text{S}$ . Presently, the  $\text{H}_2\text{S}$ -releasing properties derive from a combination of several factors such as steric hindrance, electronic effects and position of the substituents in association with the water solubility of the compounds. The aliphatic isothiocyanates (**39–45**) show a very little release of  $\text{H}_2\text{S}$ , when compared to the aromatic ones. Only compound **41** (hexyl isothiocyanate), identified as one of the components of the extracts from several *Brassicaceae*, showed a more relevant ability of  $\text{H}_2\text{S}$  releasing ( $C_{\text{max}} = 12.973 \mu\text{M}$ ). The relevance of the conjugation between  $-\text{SCN}$  moiety and the aromatic ring is demonstrated by the dramatic lack of  $\text{H}_2\text{S}$  releasing properties of compound **36** (benzyl isothiocyanate). As a clear consequence of the steric hindrance, the presence of any substituent in *ortho* to  $-\text{SCN}$  moiety caused a dramatic fall in the  $\text{H}_2\text{S}$  production (compounds **2**, **3**, **4**, **5**, **8**, **9**, **11**). On the other hand, the exceptions of compounds **6**, **7**, **10** and **12**, demonstrate that the presence of electron-withdrawing groups partially compensate this steric effect. When analyzing *meta*- and *para*-substituted compounds we have a clear overview of the electronic

effects deprived from the steric ones. The *meta*- and *para*- derivatives, electron-donating substituted (**13**, **14**, **16**, **20**, **26**, **27**, **32**) and electron-withdrawing substituted (**15**, **17**, **18**, **19**, **21**, **23**, **24**, **28**, **29**, **30**, **31**, **33**, **35**) are, respectively, worse and better H<sub>2</sub>S donors with respect to **1**. The poor H<sub>2</sub>S donor profile of the *o*-, *m*- and *p*-iodo substituted derivatives (**11**, **22**, **34**) is due not only to steric and reactivity factors but also to the low water solubility of the three derivatives (Table 2). The scarce water solubility may also account for the negligible H<sub>2</sub>S production of compounds **5**, **16**, **37** and **38**. On the other hand, the excellent H<sub>2</sub>S release of compound **25** arises certainly from the electron deficient nature of the pyridine ring but even the high water solubility of the compound plays an important role.

The observed behavior is strongly supported by the recently described molecular mechanism responsible for H<sub>2</sub>S release from isothiocyanates [36]. It implies a nucleophilic attack by the cysteine thiol group on the isothiocyanate moiety central carbon, leading to an ITC-cysteine adduct. An electron poor ring (such as pyridine or an electron withdrawing substituted aromatic ring) facilitates the intramolecular nucleophilic addition of the amino group leading to a 4,5-dihydrothiazole intermediate that produces H<sub>2</sub>S.

Irrespective of the mechanism of reaction, such an organic thiol-dependency of the H<sub>2</sub>S-releasing process is viewed as a particularly advantageous property, because it allows these compounds to behave as “smart” H<sub>2</sub>S-donors, able to release the gasotransmitter only in a biological environment.

Starting from the H<sub>2</sub>S-generation properties, *in silico* methods have been used in order to select the best candidate to be investigated about the cardioprotective properties.

The drug-like profile represents a critical property for assuring the advancement of a drug candidate into preclinical studies and clinical trials. Furthermore, the use of *in silico* methods to establish the potential drug-like profile for a given set of molecules, prioritizing only the most promising compounds, can limit the costs and time required for selecting potential drug candidates, also reducing the use of animals for the *in vivo* studies.

Based on this evaluation, compound **25** has been identified as suitable to proceed towards further pharmacological investigations considering both physicochemical properties, drug-like features and H<sub>2</sub>S-releasing rate.

The H<sub>2</sub>S-releasing properties of compound **25** have been firstly described by an amperometric method performed in phosphate buffer, in the presence or in the absence of L-Cys. Since the H<sub>2</sub>S-release in buffer without L-Cys is negligible, compound **25**, is expected to be relatively stable in water, but behaves as H<sub>2</sub>S-generating agent in biological systems where it can interact with endogenous organic thiols. Accordingly, as clearly highlighted in the experiments carried out with the fluorometric dye WSP-1, compound **25** was able to release H<sub>2</sub>S inside cells in a concentration-dependent manner, and this observation led to the conclusion that compound **25** shows the ability to cross the H9c2 cell membrane and release H<sub>2</sub>S at the intracellular level.

As reported for other H<sub>2</sub>S donor, in this model we evaluated the intracellular release of H<sub>2</sub>S and it is not surprising that there is not a proportional correlation between the concentration of compound **25** and the levels of the intracellular H<sub>2</sub>S release. Indeed, the H<sub>2</sub>S release could be influenced by different factors. First, the test compound must cross the cell membrane and enter the cellular environment; these processes strongly depend on the physicochemical properties of the compound. Then, the test compound (that is a thiol-dependent H<sub>2</sub>S-donor) must react with the intracellular free thiols; this reaction is strongly influenced by the compound structure and by the stoichiometric rate compound/free thiols. Therefore, a linear relationship between the extracellular concentration of the H<sub>2</sub>S-donor and the intracellular

release of H<sub>2</sub>S is not expected and can be only evaluated empirically.

Since H<sub>2</sub>S plays a pivotal role in the regulation of the vascular tone and in the cardio-protection process, the effect at the cardiac level of compound **25** has been further investigated in both *ex vivo* and *in vivo* experimental models.

Compound **25** promoted a clear vasorelaxing effect in the coronary vascular bed and effectively counteracted the coronary vasoconstriction induced by AngII.

In an *ex vivo* experimental model of myocardial I/R (Langendorff-perfused rat hearts), i.p. pre-administration of compound **25**, led to significant and evident limitation of tissue injury (the maximum effect has been measured at the dose of 20 µg.kg<sup>-1</sup>), although no clear dose-dependency was observed. Starting from the lower dose of 6.7 µg.kg<sup>-1</sup> a dose-dependent cardioprotection can be observed up to 20 µg.kg<sup>-1</sup>. But further increasing doses of compound **25**, failed to show increasing cardioprotective effects, rather increase of the ischemic area can be observed, thus indicating a weaker cardioprotective effect. This behavior can be explained by the hormesis that can be represented by a “U-shape curve”. Indeed, the hormetic effect of both H<sub>2</sub>S and isothiocyanates is widely described in the literature [46].

Regarding the vasorelaxing effect and the cardioprotection of 4-CPI and compound **25**, the different activity of the two compounds is explained by the different targets. H<sub>2</sub>S promotes vasodilation mainly by activating pharmacological targets expressed on the surface of the vascular smooth muscle cell membranes. For instance, such a vasodilation effect involves the activation of sarcolemmal K<sub>ATP</sub>, Kv7 and BKCa channels. As concerns the cardioprotective effects, they are mainly due to the activation of mitochondrial targets (i.e. to the triggering of ischemic preconditioning mechanisms). Therefore, pharmacokinetic factors (linked to the physicochemical features of the molecule) are likely to account for the differences observed in the concentration evoking vasodilator and cardioprotective effects.

Furthermore, 4-CPI 240 µg/kg exhibited a clear cardioprotective effect, but 72 µg/kg of 4-CPI failed to produce cardioprotective effects. The dose of 180 µg/kg compound **25** (equimolar dose of 4-CPI 240 µg/kg) had a similar cardioprotective effects with the 240 µg/kg of 4-CPI. However, the concentration of 20 µg/kg compound **25** exerted the maximum cardioprotective effect, while 72 µg/kg of CPI failed to produce cardioprotective effects. Although the two isothiocyanates can release H<sub>2</sub>S, they seem to behave in a different manner. The different efficacy and effect in the cardioprotection may be due to the physicochemical properties of the two compounds. The cardioprotection is mediated by intracellular channels (mitoK<sub>ATP</sub> is a main actor in mediating the cardioprotection effect of H<sub>2</sub>S). Thus, the compounds have to cross the membrane and probably 4-CPI is able to exert a more efficient vasorelaxing effect, but it is worse in crossing the membrane failing to reach the mitochondrial specific target.

Further investigations about the molecular mechanism on the cardioprotective properties of compound **25** have been carried out by evaluating the involvement of mitoK<sub>ATP</sub> channels whose activation has been previously reported to mediate beneficial effect in I/R injury models. Testai and colleagues [34] demonstrated that H<sub>2</sub>S and H<sub>2</sub>S-donors are able to activate mitoK<sub>ATP</sub> channels suggesting that they may be a main target of the anti-ischemic effects evoked by this gasotransmitter. Indeed, in our experimental model, the mitoK<sub>ATP</sub>-blocker 5-HD (10 mg.Kg<sup>-1</sup>) almost completely abolished the effects of compound **25**, strongly suggesting that mitoK<sub>ATP</sub> is likely to be involved in the cardioprotective effects of H<sub>2</sub>S.

The “bi-modal” curve is reflected also by the measurement of LDH activity in the perfusate effluent, confirming the tissue damage highlighted by the morphometric analysis.

Finally, the cardioprotective effects of compound **25** were tested *in vivo*, in an experimental model of acute myocardial infarction in rats, more closely resembling the clinical pattern of myocardial infarction. Also, in this model, compound **25** ( $20 \mu\text{g}\cdot\text{kg}^{-1}$ ) exhibited cardioprotective effects.

## Conclusion

A library of forty-five isothiocyanates was evaluated for its ability to release  $\text{H}_2\text{S}$  and then, by an *in silico* approach, compound **25** was identified as the most promising one. This derivative was thoroughly characterized for its cardioprotective function by means of *ex vivo* and *in vivo* assays. In conclusion, our results strongly suggest that isothiocyanate-based  $\text{H}_2\text{S}$ -releasing drugs, such as compound **25**, can trigger a “pharmacological pre-conditioning” and could represent a suitable pharmacological option in anti-ischemic therapy.

## Compliance with Ethics Requirements

All Institutional and National Guidelines for the care and use of animals (fisheries) were followed.

## Funding

This study was supported by the Italian Ministry of University and Research (MIUR) PRIN 2017XP72RF - Hydrogen Sulfide in the Vascular Inflammation-Aging: role, therapeutic Opportunities and development of novel pharmacological tools for age-related cardiovascular diseases (SVAgO).

## Declaration of Competing Interest

The authors have declared no conflict of interest.

## References

- [1] Wallace JL, Wang R. Hydrogen sulfide-based therapeutics: exploiting a unique but ubiquitous gasotransmitter. *Nat Rev Drug Discov* 2015;14(5):329–45.
- [2] Kamoun P. Endogenous production of hydrogen sulfide in mammals. *Amino Acids* 2004;26(3):243–54.
- [3] Shibuya N, Tanaka M, Yoshida M, Ogasawara Y, Togawa T, Ishii K, et al. 3-Mercaptopyruvate sulfurtransferase produces hydrogen sulfide and bound sulfane sulfur in the brain. *Antioxid Redox Signal* 2009;11(4):703–14.
- [4] Miyamoto R, Otsuguro K, Yamaguchi S, Ito S. Contribution of cysteine aminotransferase and mercaptopyruvate sulfurtransferase to hydrogen sulfide production in peripheral neurons. *J Neurochem* 2014;130(1):29–40.
- [5] Stipanuk MH. Sulfur amino acid metabolism: pathways for production and removal of homocysteine and cysteine. *Annu Rev Nutr* 2004;24:539–77.
- [6] Brancaleone V, Esposito I, Gargiulo A, Velleco V, Asimakopoulou A, Citi V, et al. D-Penicillamine modulates hydrogen sulfide ( $\text{H}_2\text{S}$ ) pathway through selective inhibition of cystathionine-gamma-lyase. *Br J Pharmacol* 2016;173(9):1556–65.
- [7] Corvino A, Severino B, Fiorino F, Frecentese F, Magli E, Perissutti E, et al. Fragment-based de novo design of a cystathionine gamma-lyase selective inhibitor blocking hydrogen sulfide production. *Sci Rep* 2016;6:34398.
- [8] Geng B, Yang J, Qi Y, Zhao J, Pang Y, Du J, et al.  $\text{H}_2\text{S}$  generated by heart in rat and its effects on cardiac function. *Biochem Biophys Res Commun* 2004;313(2):362–8.
- [9] Calvert JW, Jha S, Gundewar S, Elrod JW, Ramachandran A, Pattillo CB, et al. Hydrogen sulfide mediates cardioprotection through Nrf2 signaling. *Circ Res* 2009;105(4):365–74.
- [10] Costa AD, Garlid KD, West IC, Lincoln TM, Downey JM, Cohen MV, et al. Protein kinase G transmits the cardioprotective signal from cytosol to mitochondria. *Circ Res* 2005;97(4):329–36.
- [11] Testai L, Marino A, Piano I, Brancaleone V, Tomita K, Di Cesare Mannelli L, et al. The novel  $\text{H}_2\text{S}$ -donor 4-carboxyphenyl isothiocyanate promotes cardioprotective effects against ischemia/reperfusion injury through activation of mitoKATP channels and reduction of oxidative stress. *Pharmacol Res* 2016;113(Pt A):290–9.
- [12] Rose P, Dymock BW, Moore PK. GYY4137, a novel water-soluble,  $\text{H}_2\text{S}$ -releasing molecule. *Methods Enzymol* 2015;554:143–67.
- [13] Severino B, Corvino A, Fiorino F, Luciano P, Frecentese F, Magli E, et al. 1,2,4-Thiadiazolidin-3,5-diones as novel hydrogen sulfide donors. *Eur J Med Chem* 2018;143:1677–86.
- [14] Martelli A, Testai L, Citi V, Marino A, Pugliesi I, Barresi E, et al. Arylthioamides as  $\text{H}_2\text{S}$  donors: L-cysteine-activated releasing properties and vascular effects in vitro and in vivo. *ACS Med Chem Lett* 2013;4(10):904–8.
- [15] Barresi E, Nesi G, Citi V, Piragine E, Piano I, Taliani S, et al. Iminothioethers as hydrogen sulfide donors: from the gasotransmitter release to the vascular effects. *J Med Chem* 2017;60(17):7512–23.
- [16] Mitidieri E, Tramontano T, Gurgone D, Citi V, Calderone V, Brancaleone V, et al. Mercaptopyruvate acts as endogenous vasodilator independently of 3-mercaptopyruvate sulfurtransferase activity. *Nitric Oxide* 2018;75:53–9.
- [17] Ercolano G, De Cicco P, Frecentese F, Saccone I, Corvino A, Giordano F, et al. Anti-metastatic properties of naproxen-HBTA in a murine model of cutaneous melanoma. *Front Pharmacol* 2019;10:66.
- [18] Citi V, Martelli A, Testai L, Marino A, Breschi MC, Calderone V. Hydrogen sulfide releasing capacity of natural isothiocyanates: is it a reliable explanation for the multiple biological effects of Brassicaceae? *Planta Med* 2014;80(8–9):610–3.
- [19] Lucarini E, Micheli L, Trallori E, Citi V, Martelli A, Testai L, et al. Effect of glucoraphanin and sulforaphane against chemotherapy-induced neuropathic pain: Kv7 potassium channels modulation by  $\text{H}_2\text{S}$  release in vivo. *Phytother Res* 2018;32(11):2226–34.
- [20] Martelli A, Testai L, Citi V, Marino A, Bellagambi FG, Ghimenti S, et al. Pharmacological characterization of the vascular effects of aryl isothiocyanates: is hydrogen sulfide the real player? *Vascul Pharmacol* 2014;60(1):32–41.
- [21] Sestito S, Daniele S, Pietrobono D, Citi V, Bellusci L, Chiellini G, et al. Memantine prodrug as a new agent for Alzheimer's Disease. *Sci Rep* 2019;9(1):4612.
- [22] Rapposelli S, Gambari L, Digiacoio M, Citi V, Lisignoli G, Manferdini C, et al. A Novel  $\text{H}_2\text{S}$ -releasing Amino-Bisphosphonate which combines bone anti-catabolic and anabolic functions. *Sci Rep* 2017;7(1):11940.
- [23] Sestito S, Pruccoli L, Runfola M, Citi V, Martelli A, Saccomanni G, et al. Design and synthesis of  $\text{H}_2\text{S}$ -donor hybrids: a new treatment for Alzheimer's disease? *Eur J Med Chem* 2019;184:111745.
- [24] Franklin SJ, Dickinson SE, Karlage KL, Bowden GT, Myrdal PB. Stability of sulforaphane for topical formulation. *Drug Dev Ind Pharm* 2014;40(4):494–502.
- [25] Martelli A, Citi V, Testai L, Brogi S, Calderone V. Organic isothiocyanates as hydrogen sulfide donors. *Antioxid Redox Signal* 2020;32(2):110–44.
- [26] Calderone V, Martelli A, Testai L, Citi V, Breschi MC. Using hydrogen sulfide to design and develop drugs. *Expert Opin Drug Discov* 2016;11(2):163–75.
- [27] Zuber G, Frisch B, Creusat G, Thomann JS. Cationic polyethylenimine derivatives for delivering pharmacological molecules 2011. *WO 201112095..*
- [28] Elzes MR, Si G, Engbersen JFJ, Paulusse JMJ. Thiourea-functional bioadhesive poly(amido amine)s in gene delivery. *ACS Symp Ser* 2019;1309(5):93–117.
- [29] Gasser A, Brogi S, Urayama K, Nishi T, Kurose H, Tafi A, et al. Discovery and cardioprotective effects of the first non-Peptide agonists of the G protein-coupled prokineticin receptor-1. *PLoS ONE* 2015;10(4):e0121027.
- [30] Zaccagnini L, Brogi S, Brindisi M, Gemma S, Chemi G, Legname G, et al. Identification of novel fluorescent probes preventing PrP(Sc) replication in prion diseases. *Eur J Med Chem* 2017;127:859–73.
- [31] Lagorce D, Sperandio O, Baell JB, Miteva MA, Villoutreix BO. FAF-Drugs3: a web server for compound property calculation and chemical library design. *Nucleic Acids Res* 2015;43(W1):W200–7.
- [32] Peng B, Chen W, Liu C, Rosser EW, Pacheco A, Zhao Y, et al. Fluorescent probes based on nucleophilic substitution-cyclization for hydrogen sulfide detection and bioimaging. *Chemistry* 2014;20(4):1010–6.
- [33] Martelli A, Citi V, Calderone V. Vascular effects of  $\text{H}_2\text{S}$ -donors: fluorimetric detection of  $\text{H}_2\text{S}$  generation and ion channel activation in human aortic smooth muscle cells. *Methods Mol Biol* 2019;2007:79–87.
- [34] Citi V, Piragine E, Pagnotta E, Ugolini L, Di Cesare Mannelli L, Testai L, et al. Anticancer properties of erucin, an  $\text{H}_2\text{S}$ -releasing isothiocyanate, on human pancreatic adenocarcinoma cells (AsPC-1). *Phytother Res* 2019;33(3):845–55.
- [35] Testai L, D'Antongiovanni V, Piano I, Martelli A, Citi V, Duranti E, et al. Different patterns of  $\text{H}_2\text{S}/\text{NO}$  activity and cross-talk in the control of the coronary vascular bed under normotensive or hypertensive conditions. *Nitric Oxide* 2015;47:25–33.
- [36] Testai L, Strobbykina I, Semenov VV, Semenova M, Pozzo ED, Martelli A, et al. Mitochondriotropic and cardioprotective effects of triphenylphosphonium-conjugated derivatives of the diterpenoid isosteviol. *Int J Mol Sci* 2017;18(10):2060.
- [37] Lin Y, Yang X, Lu Y, Liang D, Huang D. Isothiocyanates as  $\text{H}_2\text{S}$  donors triggered by cysteine: reaction mechanism and structure and activity relationship. *Org Lett* 2019;21(15):5977–80.
- [38] Siros H, Chemi G, Gemma S, Butini S, Debyszer Z, Christ F, et al. Identification of novel 3-hydroxy-pyran-4-one derivatives as potent HIV-1 integrase inhibitors using in silico structure-based combinatorial library design approach. *Front Chem* 2019;7:574.
- [39] Siros H, Chemi G, Campiani G, Brogi S. An integrated in silico screening strategy for identifying promising disruptors of p53-MDM2 interaction. *Comput Biol Chem* 2019;83:107105.
- [40] Chemi G, Gemma S, Campiani G, Brogi S, Butini S, Brindisi M. Computational tool for fast in silico evaluation of hERG K(+) channel affinity. *Front Chem* 2017;5:7.

- [41] Lipinski CA, Lombardo F, Dominy BW, Feeney PJ. Experimental and computational approaches to estimate solubility and permeability in drug discovery and development settings. *Adv Drug Deliv Rev* 2001;46(1–3):3–26.
- [42] Gleeson MP. Generation of a set of simple, interpretable ADMET rules of thumb. *J Med Chem* 2008;51(4):817–34.
- [43] Hughes JD, Blagg J, Price DA, Bailey S, Decrescenzo GA, Devraj RV, et al. Physicochemical drug properties associated with in vivo toxicological outcomes. *Bioorg Med Chem Lett* 2008;18(17):4872–5.
- [44] Salloum FN. Hydrogen sulfide and cardioprotection—mechanistic insights and clinical translatability. *Pharmacol Ther* 2015;152:11–7.
- [45] Citi V, Piragine E, Testai L, Breschi MC, Calderone V, Martelli A. The role of hydrogen sulfide and H<sub>2</sub>S-donors in myocardial protection against ischemia/reperfusion injury. *Curr Med Chem* 2018;25(34):4380–401.
- [46] Martelli A, Piragine E, Citi V, Testai L, Pagnotta E, Ugolini L, et al. Erucin exhibits vasorelaxing effects and antihypertensive activity by H<sub>2</sub>S-releasing properties. *Br J Pharmacol* 2020;177(4):824–35.